2009 International Nuclear Atlantic Conference - INAC 2009
Rio de Janeiro,RJ, Brazil, September27 to October 2, 2009
ASSOCIAÇÃO BRASILEIRA DE ENERGIA NUCLEAR - ABEN
***ISBN:* 978-85-99141-03-8**

STUDY OF QUANTUM DOT BASED ON TIN/YTTRIUM MIXED OXIDE DOPED WITH TERBIUM TO BE USED AS BIOMARKER

Paula P. Paganini[1], Maria Claudia F. C. Felinto[1], Claudia A. Kodaira[1], Hermi F. Brito[2] and Luiz Antônio O. Nunes[3]

[1] Instituto de Pesquisas Energéticas e Nucleares, IPEN - CNEN/SP
Av. Professor Lineu Prestes 2242
05508-900 São Paulo, SP, Brazil.
paulapaganini@usp.br, mfelinto@ipen.br, claudiakodaira@yahoo.com

[2] Instituto de Química – Universidade de São Paulo, USP/São Paulo
Laboratório de Elementos do Bloco f
Av. Prof. Lineu Prestes, 748
05508-000, São Paulo, SP, Brazil.
hefbrito@iq.usp.br

[3] Instituto de Física de São Carlos – USP/São Carlos
Departamento de Física e Informática
Av. Trabalhador Sãocarlense,400
13566-590 – São Carlos, SP, Brazil.
luizant@ifsc.usp.br

ABSTRACT

Quantum dots (semiconductors nanocrystals) have brought a promising field to develop a new generation of luminescent biomarkers. The use of lanthanides ions as luminescent markers has many advantages, for example a security method, low cost, high specificity and also the luminescence can be promptly measured with high sensibility and accuracy. These luminescent dots are functionalized with biomolecules. For the luminophore particle to be connect with biologicals molecules (for example covalent antibody) is necessary a previous chemical treatment to modify luminophore particle surface and this process is called functionalization. A prior chemical treatment with changes on the surface luminophore particle is necessary to couple the luminophore to biological molecules. This process can be used as coating which can protect these particles from being dissolved by acid as well as provide functional groups for biological conjugation. This work presents a photoluminescence study of nanoparticles based on tin/yttrium mixed oxides doped with terbium ($SnO_2/Y_2O_3:Tb^{3+}$), synthesized by coprecipitation method. The nanoparticles were submitted to thermal treatment and characterized by X-Ray Powder Diffraction (XRD) that showed cassiterite phase formation and the influence of thermal treatment on nanoparticles structures. These nanoparticles going to be functionalized with a natural polysaccharide (chitosan) in order to form microspheres. These microspheres going to be irradiated with gamma radiation to sterilization and it can be evaluated if the nanoparticles are resistant to irradiation and they don't lose functionality with this process.

1. INTRODUCTION

Nanoparticles have been developed mostly to be used in a chemical and technologic field. Quantum dots studies (nanocrystal semiconductors) have brought a promising field to develop a new generation of luminescent biomarkers. [1] The luminescent biomarkers have a wide range of applications, one is biological assay to detected many different diseases. This method is fluoroimmunoassay and it is used to enzyme, antibody, cells, hormones research [2].

Since some of lanthanide ions, especially Eu^{3+} and Tb^{3+}, were found to show good luminescence characteristics (high color purity) based on the 4f electronic transitions, a variety of rare earth compounds activated by Eu^{3+} and Tb^{3+} have been studied for practical applications as phosphors [3]. Trivalent terbium ion (Tb^{3+}) doped nanocrystals have aroused vast interest due to their excellent luminescent property. Tb^{3+}-doped materials are well-known for good PL (photoluminescence) characteristics from a $^5D_4 \rightarrow {}^7F_J$ transition in the visible range [4].

The biomarkers are usually organic pigments and they show toxicity problems, short time life and large spectral profile unlike rare earth biomarkers that allow quickly measured luminescence with high sensibility and accuracy, besides they are biocompatible and nontoxic [2].

In order to connect biological molecules luminophore particle it is necessary a previous chemical treatment to modify luminophore particle surface (functionalization), once particles of rare earth oxides are water insoluble and they are dissolved by acid during activation and conjugation, losing their optical proprieties. This process can be used as coating which can protect these particles from being dissolved by acid as well as provide functional groups for biological conjugation [5].

2. EXPERIMENTAL SECTION

The mixed oxide $SnO_2/Y_2O_3:Tb^{3+}$ was prepared by neutralization of a mixing solution of tin (IV) chloride, yttrium (III) chloride and terbium chloride with ammonia solution, until pH7, in a batch reactor. The particles were aged in the solution liquor for 48h. The precipitated was very thin therefore it was opted to the migration of chloride ions using cellophane membranes where the gradient used for the separation was the difference in concentration of chloride ions in solution. For analytical control of chloride ions it was made a test with $AgNO_3$. After removal of chloride ions, the material was dried at 110 ºC in a heater. The sample thermal treatment was performed at 300, 500 and 876 ºC.

The mixed oxide was characterized by X-Ray Powder Diffraction Method (XRD) to different annealing temperatures. Crystalline phase was identified by MiniFlex II Higaku X-ray diffraction by using Cu $K\alpha$ radiation with 2θ from 5 to 80º

Steady-state excitation and emission spectra at liquid nitrogen temperatures were recorded at an angle of 22.5° (front face) with a spectrofluorimeter (SPEX-Fluorolog 2) with double grating 0.22 m monochromator (SPEX 1680), and a 450 W Xenon lamp as excitation source. All spectra were recorded using a detector mode correction.

3. RESULTS AND DISCUSSION

3.1 X-Ray Powder Diffraction

Figure. 1 shows the XRD patterns of the as-made $SnO_2/Y_2O_3:Tb^{3+}$ and heat treated at different temperatures for 1h. The as-made $SnO_2/Y_2O_3:Tb^{3+}$ is completely amorphous with noncrystalline diffraction peaks. After heat treatment, the diffraction peaks of $SnO_2/Y_2O_3:Tb^{3+}$ can be easily assigned cassiterite majority phase. [6-8] with lines of diffraction in 2θ: 26.66; 36.69; 51.78 and 64.71 referent to SnO_2, that are consistent with the data of standards ICDD (01-075-2893 and 01-088-0287). Moreover, the width of the peaks becomes sharper with higher heat-treatment temperature, which indicates the gradual formation of nanocrystal. From the obtained peak width of XRD patterns, the crystal size of $SnO_2/Y_2O_3:Tb^{3+}$ can be calculated by the Scherrer formula:

$$\mathbf{D_{hkl}} = \frac{k\lambda}{\beta cos\theta} \quad (1)$$

where D_{hkl} is the crystal size at the vertical direction of (hkl), λ is the wavelength of X-ray(Cu Kα: 1.541 Å), θ the angle of diffraction, β the full-width at half-maximum (FWHM) of the diffraction peak and the constant K is equal to 0.89.

The crystal size of $SnO_2/Y_2O_3:Tb^3$ was plotted as a function of heat-treatment temperature in Fig. 2. With the increase of heat-treatment temperature, the $SnO_2/Y_2O_3:Tb^{3+}$ nanocrystals sizes increases from about 1.7 up to 4.6 nm.

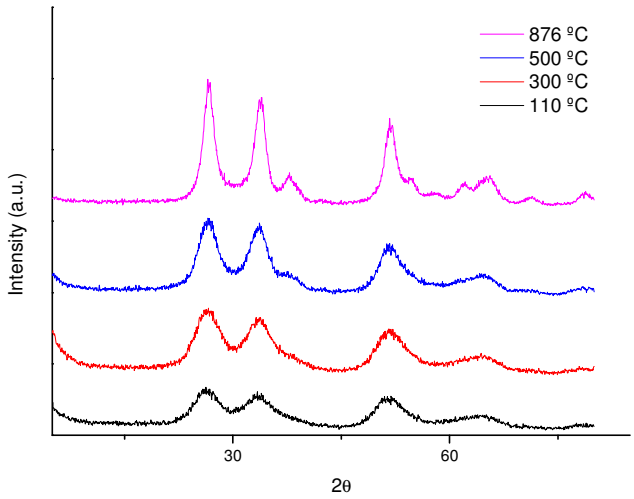

Figure 1. X-ray powder diffraction of $SnO_2/Y_2O_3:Tb^{3+}$ annealed at 110 ºC, 300 ºC, 500 ºC and 876 ºC.

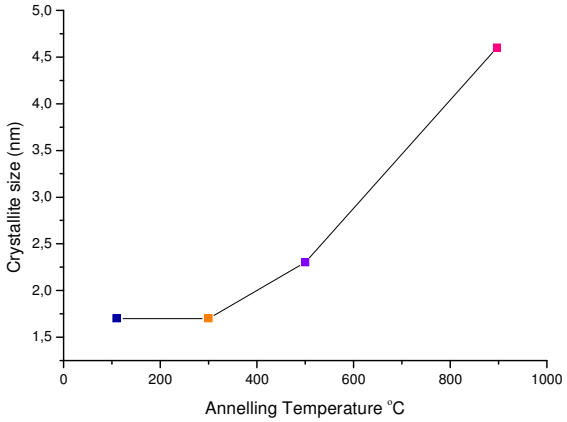

Figure 2. Crystalline size plotted against annealing temperature for $SnO_2/Y_2O_3:Tb^{3+}$

3.2 Photoluminescence study

The excitation spectrum, Fig. 3, of the $SnO_2/Y_2O_3:Tb^{3+}$ recorded at 77 K monitoring in the $^5D_4 \rightarrow {}^7F_5$ transition (544 nm) consists of a broad band in the range from 250 to 375 nm, attributed to the O→Sn semiconductor transition [9]. In addition to this band, narrow bands arising from 4f–4f transitions from the ground state $^7F_6$ level to the $^5L_9$ (349.5), $^5L_{10}$ (367), $^5G_6$ (375), $^5D_4$ (482) and to excited states levels $^5D_3 \rightarrow {}^7F_5$, $^7F_6$,423 and 449 nm, are observed. The semiconductor band with charge transfer between O→Sn are shifted to the region of lower energy, in direction of red region, with increase of annealing temperature and crystallite size. However, the relative intensity of the broad band is higher than those centered on the Tb^{3+} ion, suggesting that the indirect excitation processes of the metal ion via Sn→O semiconductor bands are more operative. It was also observed in the excitation spectra, that the structure of $SnO_2/Y_2O_3:Tb^{3+}$ exchange with the thermal treatment. The $SnO_2/Y_2O_3:Tb^{3+}$ spectra annealed at 110 and 300 ºC present the transition $^7F_6 \rightarrow {}^5L_9$ at ca 394.5nm whereas at 500 and 876 ºC these transition disappear and two new bands appear at 423 and 449 nm as commented above.

The emission spectra of $SnO_2/Y_2O_3:Tb^{3+}$, with excitation monitored at 377 nm is shown in Fig. 4. These spectra display characteristic narrow emission bands assigned to the $^5D_4 \rightarrow {}^7F_J$ transitions (J = 3, 4, 5 and 6). The strongest emissions for J=5 with maxima at around 544 nm correspond to the characteristic green emission of Tb^{3+}, $^5D_4 \rightarrow {}^7F_5$ transition, that is the most prominent which is extremely sensitive to chemical environment around this ion. The emission spectra also exhibits no bands arising from the O→Sn semiconductor transition, indicating there is an efficient intramolecular energy transfer from the matrix to the Tb^{3+} ion. Due to the shielding effect of 4f electrons by 5s and 5p electrons in outer shells in the Tb^{3+} ion, narrow emission peaks were expected, consistent with the sharp peak in Fig. 4.

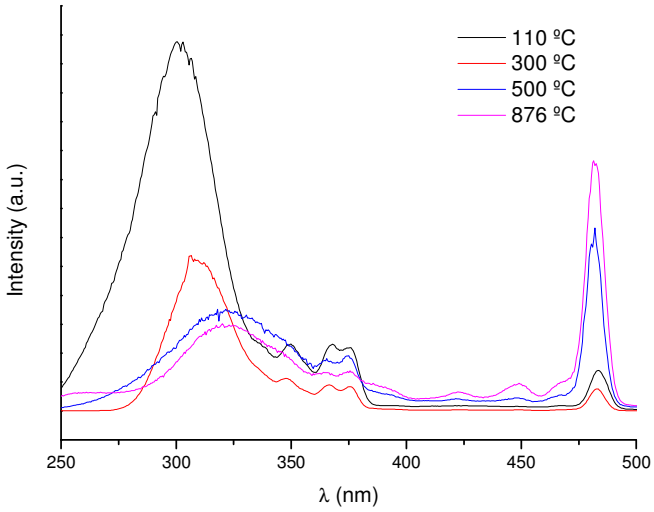

Figure 3. Excitation spectra obtained at 77K monitored at 544nm to $SnO_2/Y_2O_3:Tb^{3+}$ annealed at 110 ºC, 300 ºC, 500 ºC and 876 ºC.

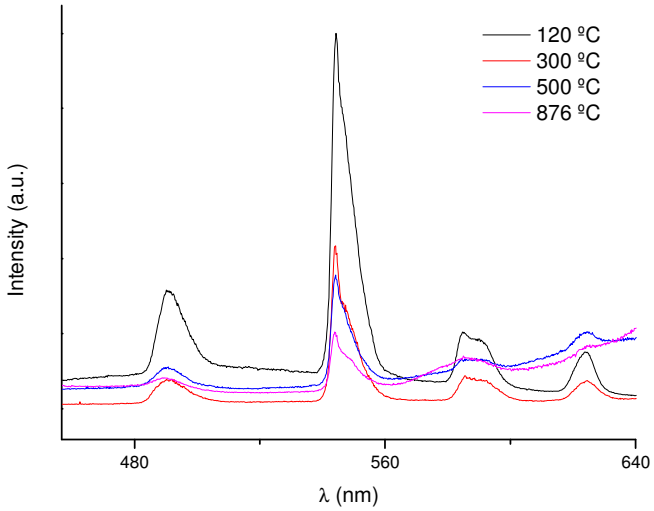

Figure 4. Comparison emission spectra obtained at 77K monitored at 377 nm to $SnO_2/Y_2O_3:Tb^{3+}$ annealed at 110 ºC, 300 ºC, 500 ºC and 876 ºC.

Fig. 5 shows the integrated intensity of green ($^5D_4 \rightarrow {}^7F_J$), are plotted as a function of heat-treatment temperature. It was also observed that, all the emission decreased with increasing of annealing temperature and until 500 ºC the PL intensity of $^5D_4 \rightarrow {}^7F_5$ transition (green component) dominates that of $^5D_4 \rightarrow {}^7F_3$ one (red component) [10,11].

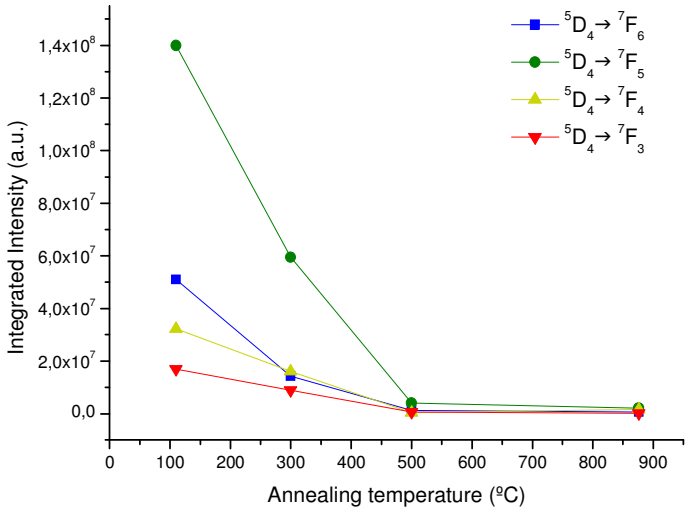

Figure 5. Evolution versus annealing temperature of the integrated PL intensities relatives to the $^5D_4 \rightarrow ^7F_J$ (J=6-3) transitions of terbium in $SnO_2/Y_2O_3:Tb^{3+}$ (emission spectra obtained at 77K monitored excitation at 377 nm).

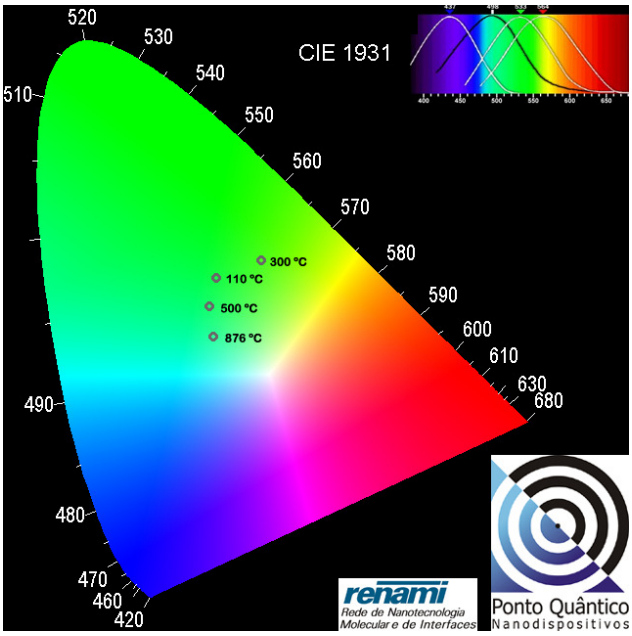

Figure 6. CIE (x,y) diagram displaying emission color coordinates of $SnO_2/Y_2O_3:Tb^{3+}$ annealed at 110 ºC, 300 ºC, 500 ºC and 876 ºC. excited at 377 nm (room temperature).

Colour purity can be visualized in the chromaticity diagram (Fig. 6), as blue, red, and green vertex regions, with the emission colour coordinates of the luminescent material. The CIE

(Comission Internacionale de l'Eclairage) chromaticity diagram of $SnO_2/Y_2O_3:Tb^{3+}$ sample at different temperature were obtained using a Spectra Lux Software v.2.0 Beta [12]. For any given colour there is one setting for each three numbers X, Y and Z known as tristimulus values that will produce a match [13,14]. Based on emission spectra of $SnO_2/Y_2O_3:Tb^{3+}$ samples, the (x,y) colour coordinates were determined with the following values (x,y) = (0.27, 0.48), (0.34, 0.50), (0.26, 0.44) and (0.27, 0.39) for the samples heated at different temperatures 110, 300, 500 and 876 °C, respectively.

4. CONCLUSIONS

Nanostructured Tb^{3+}-doped SnO_2/Y_2O_3 particles have been synthesized using a modified sol-gel method. X-ray powder diffraction show the $SnO_2/Y_2O_3:Tb^{3+}$ can be easily assigned cassiterite majority phase. It was found the increasing of SnO_2/Y_2O_3 crystal size with the annealing temperature. The PL emission intensities of $^5D_4 \rightarrow {}^7F_J$ (J = 6–3) transitions of Tb^{3+} ions were dependent on the annealing temperature. Additionally, the $SnO_2/Y_2O_3:Tb^{3+}$ is a potential candidate as emitter in photonic systems.

ACKNOWLEDGMENTS

The authors acknowledge to Cordenação de Aperfeiçoamento de Pessoal de Nível Superior (CAPES), Conselho Nacional de Desenvolvimento Científico e Tecnológico (CNPq), Fundação de Amparo à Pesquisa do Estado de São Paulo (FAPESP) Rede de Nanotecnlogia Molecular e Interfaces(RENAMI), Instituto Nacional de Ciência e Tecnologia de Nanotecnologia para Marcadores Integrados (INCT-INAMI) for financial support. They also acknowledge IPEN`s Laboratories.

REFERENCES

1. S. Santra; P. Zhang; K. Wang; R. Tapec and W. Tan, "Conjugation of biomolecules with luminophore-doped silica nanoparticles for photostable biomarkes." *Analytical Chemistry*, **v.73**, pp.4988-4993 (2001).
2. T. S. Martins and P. C. Isolani, "Terras raras: aplicações industriais e biológicas." *Química Nova*, **v.28**, pp.111-117 (2005).
3. L.J. Bian, H.A. Xi, X. F. Qian, J. Yin, Z. K. Zhu, Q. H. Lu. "Synthesis and luminescence property of rare earth complex nanoparticles dispersed within pores of modified mesoporous silica." *Materials Research Bulletin,* **v.37** pp.2293-2301 (2002).
4. E. E. S.Teotonio, G M Fett; H. F. Brito; A. C Trindade,; M. C. F. C. Felinto, "Novel unexpected Tb^{3+} coordination polymer containing two carboxylate ligands: Syntheses, structure and photoluminescent properties." *Inorganic Chemistry Communications*, **v.10**, pp.867-872 (2007).
5. J. Feng; G. Shan; A. Maquieira; M. E. Koivunen; B. Guo; B. D. Hammock and I. M. Kennedy, "Functionalized Europium Oxide Nanoparticles Used as a Fluorescent Label in an Immunoassay for Atrazine." *Anal. Chem.* **v.75**, pp. 5282–5286 (2003).

6. D. Cai; Y. Sut, Y. Chen; J. Jiang, Z. He and L. Chen, "Synthesis and photoluminescence properties of novel SnO_2 asterisk-like nanostructures." *Materials Letters*, **v. 59**, pp.1984 – 1988 (2005).
7. P. M. Kumar, S. Badrinarayanan and M. Sasatry. "Nanocrystalline TiO_2 studied by optical, FTIR and X-ray photoelectron spectroscopy: correlation to presence of surface states." *Thin Solid Films*, **v. 358**, pp.122-130 (2000).
8. L. Zhao, J. Yu and B. Cheng. "Preparation and characterization os SiO_2/TiO_2 composite microspheres with microporous SiO_2 core/mesoporous TiO_2 shell." *Journal of Solid State Chemistry*, **v. 178**, pp.1818-1824 (2005).
9. C. A. Kodaira, H. F. Brito, O. L. Malta and O. A. Serra**.** "Luminescence and energy transfer of the europium (III) tungstate obtained via the Pechini method." *J.Lumin*, **v.101**, pp.11-21 (2003)
10. H. Song, J. Wang, "Dependence of photoluminescent properties of cubic Y_2O_3:Tb^{3+} nanocrystals on particle size and temperature." *J. Lumin*., **v.118**, pp.220–226 (2006).
11. J. H. Park, N. G. Back, M. G. Kawak, B. E. Jun, B. C. Choi, B. K. Moon, J. H. Jeong, S. S. Yi and J. B. Kim, "Synthesis and properties of luminescencent Y_2O_3: Tb^{3+} (5, 8, 12 wt.%) nanocrystals." *Mate. Sci. Eng C.* **v.27**, pp. 998–1001 (2007).
12. P. A. Santa-Cruz, F. S. Teles, Spectra Lux Software v.2.0 Beta, Ponto Quântico Nanodispositivos, RENAMI, 2003.
13. K. M. N. K. Prasad, S. Raheem, P. Vijayalekshmi, C. K. Sastri, "Basic aspects and applications of tristimulus colorimetry." *Talanta* **v.43,** pp.1187-1206 (1996)
14. A. S. Maia, R. Stefani, C. A. Kodaira, M. C. F. C. Felinto, E. E. S. Teotonio, H. F. Brito, "Luminescent nanoparticles of MgAl2O4:Eu,Dy prepared by citrate sol–gel method." *Optical Materials* **v.31** pp.440–444 (2008)